STRUCTURAL CONTROL AND HEALTH MONITORING
Struct. Control Health Monit. 2015; 22:139–151
Published online 8 May 2014 in Wiley Online Library (wileyonlinelibrary.com). DOI: 10.1002/stc.1665

Retest of Neoprene seismic isolation bearings after 30 years

Niel C. Van Engelen[1,2,*,†] and James M. Kelly[1]

[1]Pacific Earthquake Engineering Research Center, University of California Berkeley, Richmond, CA, 94804-4698, USA
[2]Department of Civil Engineering, McMaster University, Hamilton, Ontario Canada L8S 4L7

SUMMARY

This paper describes the retest of a set of Neoprene (Polychloroprene) steel reinforced elastomeric isolator bearings that were originally tested as part of an experimental program in 1981. The original bearings were tested on a shake table as a demonstration of the feasibility of base isolation for the seismic protection of buildings. Two types of bearings were provided, and not all were used. The unused bearings were stored unloaded at room temperature for over 30 years. Although there has been a very substantial improvement in the number and quality of the instrumentation available to the test program over the span of 30 years, it is possible to compare the results of relatively similar shake table tests on the bearings. The shake table tests are used to assess the changes in the horizontal stiffness and damping values for the bearings over this period. Copyright © 2014 John Wiley & Sons, Ltd.

Received 7 November 2013; Revised 24 February 2014; Accepted 10 April 2014

KEY WORDS: Neoprene; aging; base isolation; steel reinforced; elastomeric isolators

1. INTRODUCTION

Neoprene (Polychloroprene) is used extensively worldwide for thermal expansion bridge bearings, but it is not very common in seismic isolation bearings for buildings. It has been used in several isolation projects in Yerevan, Armenia, for a number of multi-family apartment buildings and condominiums with a locally manufactured compound and bearing [1]. The sole other use of Neoprene bearings is in a number of French nuclear facilities. It is a surprising fact that the only nuclear power plants that use seismic isolation are built on Neoprene isolation bearings. These facilities include the Cruas-Meysse nuclear power plant located in the south of France on the Rhone River, shown in Figure 1. It is a four-unit 3600 MW plant built by EDF, completed in 1984, on 3600 bearings; 900 for each unit. The square bearings used in this project have a length of 19.7 in. (500 mm), and the system provides an isolation period of 1 s [2].

Another example of a French nuclear facility on Neoprene isolators is the La Hague Spent Fuel Storage Pools building built by Areva. The system is composed of square bearings with a length of 27.6 in. (700 mm) that provide an isolation period of 1.2 s. The Jules Horowitz Reactor, an experimental and medical research reactor at the CEA research site at Cadarache, France, is isolated with 195 square bearings, which have a length of 35.4 in. (900 mm). Also, presently under construction at the Cadarache site is a new experimental fusion reactor, a Tokamak called ITER, which is isolated with 493 Neoprene bearings with the same dimensions and mechanical properties as those of the Jules Horowitz Reactor. At this time, the foundations and the isolation system are in place. These French nuclear facilities use a Neoprene compound with a shear modulus of 160 psi (1.1 MPa) and a

*Correspondence to: Niel C. Van Engelen, Department of Civil Engineering, McMaster University, 1280 Main St. West, Hamilton, Ontario, Canada L8S 4L7.
†E-mail: vanengn@mcmaster.ca

Figure 1. The Cruas-Meysse nuclear power plant, France.

conservatively estimated, for design purposes, equivalent viscous damping of 6–7%. The aging of this compound has been studied extensively using accelerated aging tests following the Arrhenius approach [3].

Because the functionality and performance of a seismic isolation system is primarily related to a low horizontal stiffness, the main emphasis on the evolution with time is the shear modulus. It is accepted that the favorable properties of elastomeric isolators degrade with time as the elastomer hardens and becomes brittle because of reactions with the environment, such as oxidation. Consequently, concern over the sensitivity of an elastomeric isolation system to aging is amplified because of uncertainty in the aged performance and the inherent long design life of structures, which span many decades. Inadequate knowledge of the aging effect on elastomeric isolators may increase the financial burden of the isolation system because of the premature partial or full replacement of a functional system.

The exterior surface of the isolator is most affected by aging because of the higher level of exposure to the environment and subsequent oxidation. The region with the largest variation in material properties occurs at the exterior surface of the isolator. The variation in material properties gradually decreases moving inwards from the exterior surface to the interior region of the elastomer, which may not be affected by oxidation. The permeability of the exterior oxidized region is substantially reduced, which acts as a mechanism to prevent further oxidation of the interior region of the isolator [4]. Intuitively, smaller isolators are more sensitive to aging because of the larger ratio of exterior surface area to the volume of the elastomer. This was demonstrated experimentally through accelerated aging by Yura et al. [5] for Shore A 50 and 70 durometer natural rubber and Neoprene specimens. The study considered three different sizes of square specimens with lengths between 1 in. (25.4 mm) and 3 in. (76.2 mm). The accelerated aging caused an increase in stiffness up to about 60% at a shear strain of 0.5 depending on the hardness and the size of the specimen. Translating the accelerated aging to natural aging at ambient temperatures, the study concluded that it would take hundreds of years for the observed increase to occur through natural aging at ambient temperatures.

Coladant [6] investigated the aging of Neoprene isolators utilized in the Cruas-Meysse nuclear power plant. After approximately 11 years of natural aging, the shear modulus increased by about 25%. From the limited data available, it was predicted that the shear modulus would increase by a maximum of 37% over the expected lifespan. Accelerated aging tests on samples of the compound were also carried out. The samples were placed in a heated chamber at 70 °C for 10 weeks with samples regularly tested for the dynamic modulus and damping. During these tests the modulus increased at most by 25% and the damping decreased by about 10%.

Russo et al. [7] considered the accelerated aging of unbonded fiber reinforced Neoprene elastomeric isolators. It was noted that the code used for the accelerated aging did not indicate the representative age of the treated specimens. A maximum increase in horizontal stiffness of 17% at a shear strain of 1.0 and a maximum decrease in equivalent viscous damping of 20% were observed in the study.

In this paper, the effective horizontal stiffness and equivalent viscous damping of aged Neoprene annular steel reinforced elastomeric isolators (SREIs) is investigated. The Neoprene SREIs considered were manufactured and tested in an experimental study to demonstrate the feasibility of base isolation as a means of seismic protection for buildings over 30 years ago [8]. The results from the original study

DOI: 10.1002/stc

are reviewed, and a similar experimental program was conducted on a base isolated structure with six previously untested SREIs from the original study. The SREIs were aged unloaded at room temperature for approximately 31 years as shown in Figure 2. The horizontal properties are compared with the original study and investigated for retention of favorable seismic isolation characteristics over this period.

2. REVIEW OF THE 1981 TESTING

The original experimental program presented in Kelly and Hodder [8] was conducted to demonstrate the viability of seismic isolation for structures and the suitability of elastomeric isolators. This was demonstrated through a series of shake table experiments on a scaled model with the addition of static testing to investigate the horizontal and vertical properties of the annular isolators. The one-third scale model used in the shake table experiments was a five-story three-by-one bay steel frame. Each of the four corners of the steel frame was supported on a bearing, and base floor girders connected the unsupported columns to the bearings. The total weight of the model was 80 kip (356 kN), which includes the self-weight of the frame and additional dead load.

2.1. Specimens

The central hole of the annular isolators was provided to facilitate the use of elastomeric and lead cores in the original study; only the properties of the unfilled configuration are considered for comparative purposes. The isolators were designed by the Polymer Products Department, Elastomers Division of E.I. du Pont de Nemours & Co. (Inc.), in Wilmington, Delaware, and manufactured and donated by Oil States Industries Inc., in Athens, Texas.

Two Neoprene elastomers were used: one with a Shore A 40 durometer hardness and the other with a 50 durometer hardness, henceforth referred to as 40A and 50A isolators. The multi-layer isolators were manufactured with 44 layers of elastomer and 43 layers of steel reinforcement. Each layer of Neoprene was approximately 0.057 in. (1.4 mm) thick, and the total thickness of the elastomeric layers was 2.5 in. (63.5 mm). Each layer of steel reinforcement was approximately 0.06 in. (1.5 mm) thick. Two square steel end plates, each with a thickness of 0.25 in. (6.4 mm) and a width and length of 7 in. (177.8 mm), were used to mechanically fasten the isolator to the substructure and superstructure. The total height of the isolator was 5.5 in. (139.7 mm). The outer diameter was 5.5 in. (139.7 mm), and the inner diameter was 2.0 in. (50.8 mm). The annular isolators had a total plan area of 20.6 $in.^2$ (13,290 mm^2). Figure 3 shows a cross section of a specimen emphasizing the moderate shape factor of 15.4 represented by the thin layers of elastomer in comparison with the loaded area.

2.2. Static testing

The isolators were initially statically tested in tandem and with unfilled cores. A vertical compressive force of 20 kip (89.0 kN) was applied corresponding to the average weight on each isolator in the

Figure 2. Isolator storage conditions.

DOI: 10.1002/stc

Figure 3. Cross section of an annular steel reinforced elastomeric isolator specimen.

experimental model. The horizontal stiffness of a single 50A isolator was approximately 1.0 kip/in. (0.175 kN/mm) at zero horizontal displacement. It was observed that the horizontal stiffness steadily decreased with increasing displacement to 0.4 kip/in. (0.070 kN/mm) at a horizontal displacement of 2.0 in. (50.8 mm). The static vertical stiffness under a vertical compressive force of 20.0 kip (89.0 kN) was 420 kip/in. (74 kN/mm) and 600 kip/in. (105 kN/mm) for the 40A and 50A isolator, respectively. A critical load of 33.4 kip (149 kN) was experimentally determined at zero horizontal displacement for the 40A isolator. This was 38% lower than the critical load of 53.8 kip (239 kN) carried by the 50A isolator. The load deflection curves for the static compression tests can be reviewed in Kelly and Hodder [8].

2.3. Dynamic testing

The dynamic shake table test program considered four historic California earthquake records, which occurred prior to 1981. The earthquake records were complimented with numerous pullback tests where the model was initially displaced and suddenly released in free vibration. From the pullback tests, a fixed base fundamental frequency of 3.9 Hz was determined. The fundamental frequency of the model, base isolated with 40A and 50A isolators, was 0.50 and 0.75 Hz, respectively. On the basis of the fundamental frequency, the horizontal stiffness of the 40A isolators was determined to be 0.50 kip/in. (0.088 kN/mm) and 1.15 kip/in. (0.201 kN/mm) for the 50A isolators. It was noted that the dynamically obtained horizontal stiffness for the 50A isolator was 15% higher than determined statically at zero horizontal displacement.

Horizontal force-displacement cycles at the peak isolator displacement of the model in the Imperial Valley (1940) El Centro record at a peak ground acceleration (PGA) of 0.54 g, reproduced from Kelly and Hodder [8], are presented in Figure 4. The equivalent viscous damping of the system was 11% and 10% for the 40A and 50A isolators, respectively. In all cases, the isolation mode dominated the response of the model and the structure responded in near rigid motion on top of the isolation system. The fixed base structure amplified the table acceleration of 0.54 g to a peak absolute acceleration of 1.9 g at the fifth floor of the structure. Both the 40A and 50A isolation systems resulted in a substantial decrease in peak absolute acceleration. The 40A isolator, which had a lower horizontal stiffness, provided a larger decrease in peak absolute acceleration to 11% of the table acceleration. The 50A isolator had a peak absolute acceleration of roughly 0.1 g or 19% of the table acceleration. Similar large decreases in peak absolute acceleration of the structure were obtained for the other earthquake records considered.

The maximum displacement capacity of the 50A isolators was evaluated by increasing the peak table acceleration to 0.68 and 0.835 g. The peak displacement was 2.5 in. (63.5 mm) at a peak table acceleration of 0.54 g. By increasing the peak table acceleration to 0.68 g, the peak displacement

DOI: 10.1002/stc

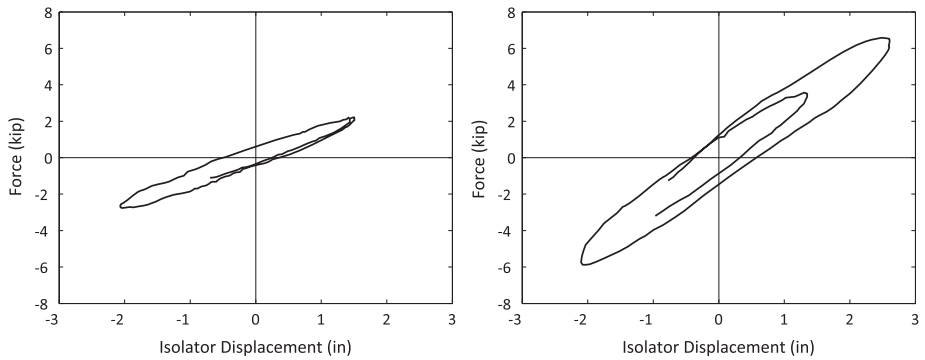

Figure 4. Peak isolator displacement hysteresis loops from the El Centro record (PGA = 0.54 g) of the (a) 40A and (b) 50A isolators.

increased to 3.5 in. (88.9 mm), but the peak absolute acceleration of the frame was relatively unaffected. At the maximum considered table acceleration of 0.835 g, the peak displacement was 4.2 in. (106.7 mm), and only a minor increase in the peak absolute acceleration of the frame was observed. The small change in peak absolute acceleration of the frame was attributed to a favorable softening and increase in damping in the isolators. This softening and increase in damping, as shown in Figure 5, was larger where an increase in vertical compressive force occurred because of overturning moments. The horizontal stiffness of SREIs decreases with increasing horizontal displacement [10]. Although significant critical load carrying capacity exists as the horizontal displacement approaches the diameter of the bearing, the combination of large displacements and increased vertical compressive force amplifies the softening [11]. Consequently, under these conditions, the isolator approaches the stability limit as observed in the Southwest isolator.

3. EXPERIMENTAL TESTING

3.1. Experimental apparatus

The experimental tests were conducted on a single degree of freedom stiff platform assembly on a linear bearing system. The one-third scale superstructure was a two-story two-by-one bay steel frame assembled from the NEES REPEAT system with a total weight of 87 kip (387 kN) including the additional dead load. Six isolators were considered simultaneously, one under each column of the frame, the isolator layout is provided in Figure 6. This differs from the original experiment, which

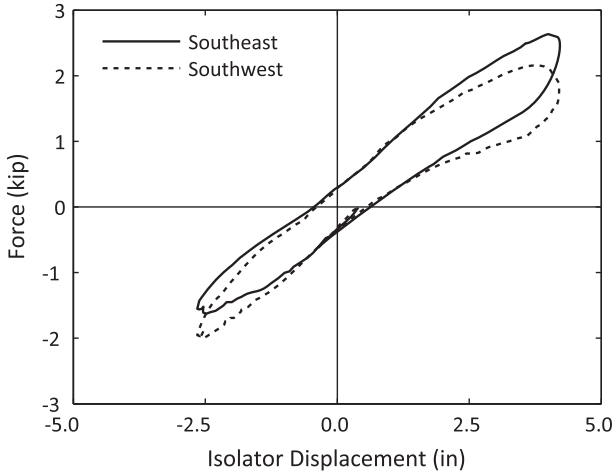

Figure 5. Comparison of the hysteresis loops from the El Centro record (PGA = 0.835 g) of the Southeast and Southwest isolators.

DOI: 10.1002/stc

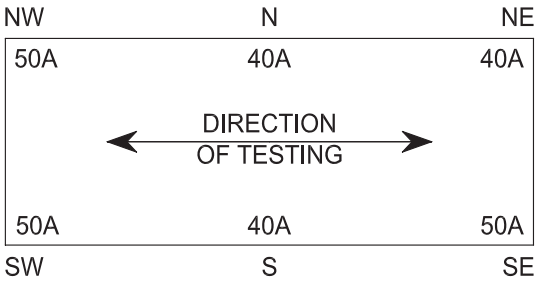

Figure 6. Isolator layout.

was isolated with four 40A or four 50A bearings. The average vertical compressive force of 14.5 kip (64.5 kN) per isolator was 73% of the average vertical compressive force applied to each isolator in the original study. Each specimen was mechanically fixed on top of a five component load cell as shown in Figure 7a. The experiments were conducted with a rigid and flexible superstructure configuration. The rigid configuration was implemented by utilizing the safety system to stiffen the superstructure. In the flexible configuration, the safety system was used only to prevent the potential collapse of the superstructure. The experimental model is shown in Figure 7b.

3.2. Test program

The experimental test program consisted of pullback tests, historical earthquake records, and acceleration sinusoidal sweeps. Only the pullback tests and Imperial Valley (1940) El Centro Array #9 record results were considered for comparison with the original study. The portions of the experimental program considered in this study are summarized in Table I. The pullback tests were conducted by instantaneously releasing the isolation level of the structure from an initial displacement of 1.0 in. (25.4 mm), 1.2 in. (30.5 mm), 1.5 in. (38.1 mm), and 2.0 in. (50.8 mm) and monitoring the free vibration response. Seven pullback tests, four in the rigid configuration and three in the flexible configuration, were considered. Fourteen experiments were conducted with the El Centro record, eight in the rigid configuration and six in the flexible configuration. The recorded experimental PGA of the El Centro records ranged from 0.15 to 0.67 g and 0.16 to 0.61 g for the rigid and flexible configuration, respectively. Numerous additional experiments with the other earthquake records were conducted intermittently between the considered experiments. The Southwest 50A isolator was replaced at the end of the flexible configuration experiments because of an observed delamination. Additional

(a) (b)

Figure 7. Experimental apparatus showing (a) a steel reinforced elastomeric isolator specimen mechanically fixed to the supports and (b) the steel frame (blue) and additional dead load (white).

DOI: 10.1002/stc

Table I. Experimental program.

Configuration	Experiment	Amplitude
Rigid	Pullback	1 in. (25.4 mm)
	Pullback	1.2 in. (30.5 mm)
	Pullback	1.5 in. (38.1 mm)
	El Centro (1940)	0.15 g
	El Centro (1940)	0.21 g
	El Centro (1940)	0.37 g
	El Centro (1940)	0.45 g-A
	El Centro (1940)	0.54 g-A
	El Centro (1940)	0.54 g-B
	El Centro (1940)	0.67 g
	El Centro (1940)	0.65 g
	Pullback	1.5 in. (38.1 mm)
Flexible	Pullback*	1.5 in. (38.1 mm)
	El Centro (1940)	0.16 g
	El Centro (1940)	0.22 g
	El Centro (1940)	0.34 g
	El Centro (1940)	0.45 g-B
	El Centro (1940)	0.52 g
	El Centro (1940)	0.61 g
	Pullback	1.5 in. (38.1 mm)
	Pullback	2.0 in. (50.8 mm)

*Southwest isolator replaced.

experiments, including pullback, historical earthquake records, and acceleration sinusoidal sweeps, were conducted after the final El Centro record considered in this study.

4. COMPARISON BETWEEN ISOLATORS

4.1. 40A isolators

Figure 8a shows the effective horizontal stiffness, k_{eff}, of the rigid and flexible configurations as a function of the peak isolator displacement of the El Centro records. The effective horizontal stiffness presented was determined from the cycle over which the peak isolator displacement occurred. The minimum peak isolator displacement was 0.39 in. (9.9 mm), and the maximum peak isolator displacement was 3.01 in. (76.5 mm) at a PGA of 0.15 and 0.67 g, respectively. A softening trend occurred with increasing peak isolator displacement. A maximum effective horizontal stiffness of 0.91 kip/in. (0.159 kN/mm) occurred at the minimum peak isolator displacement of 0.39 in. (9.9 mm) in the Northeast isolator. The effective horizontal stiffness decreased by 35% to a minimum stiffness of

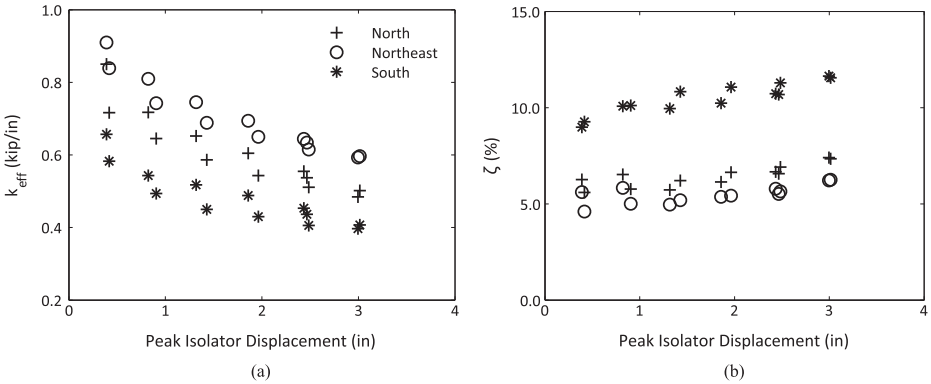

Figure 8. Comparison of the (a) effective horizontal stiffness and (b) the equivalent viscous damping as a function of peak isolator displacement obtained from the El Centro records for the 40A isolators.

DOI: 10.1002/stc

0.59 kip/in. (0.103 kN/mm) at the maximum peak isolator displacement of 3.01 in. (76.5 mm). Similar to the Northeast isolator, the effective horizontal stiffness of the South isolator decreased over the range of peak isolator displacement by 36% from 0.66 kip/in. (0.116 kN/mm) to 0.40 kip/in. (0.070 kN/mm). The effective horizontal stiffness varied significantly between the three 40A isolators. The mean, μ, and coefficient of variation, c_v, are provided in Table II at all levels of peak isolator displacement. The c_v is relatively consistent, ranging between 0.16 and 0.21, but is representative of the large variation observed in the effective horizontal stiffness.

The equivalent viscous damping, ζ, was found to increase with increasing peak isolator displacement as shown in Figure 8b. The South isolator, which had the lowest horizontal stiffness, had the highest damping ranging from 9.0% to 11.6% at 0.39 in. (9.9 mm) and 3.01 in. (76.5 mm), respectively. The damping in the South isolator was considerably higher than the North or Northeast isolator, which varied between 4.6% at 0.39 in. (9.9 mm) in the Northeast isolator and 7.4% at 3.01 in. (76.5 mm) in the North isolator. Figure 9 highlights the difference in effective horizontal stiffness and damping between the Northeast and South isolator. The higher damping in the South isolator is partially attributed to the lower effective horizontal stiffness. However, from the hysteresis loops, it was observed that the area enclosed within the loops was 26% greater for the South isolator. This suggests that the energy dissipation characteristics of the South isolator were greater than the Northeast or North isolators.

Table II. Mean and coefficient of variation of the effective horizontal stiffness obtained from the El Centro record.

PGA	Peak displacement		40A			50A		
(g)	(in.)	(mm)	μ (kip/in.)	μ (kN/mm)	c_v	μ (kip/in.)	μ (kN/mm)	c_v
0.15	0.39	9.9	0.81	0.141	0.16	1.69	0.297	0.03
0.16	0.42	10.7	0.71	0.125	0.18	1.54	0.271	0.06
0.21	0.82	20.8	0.69	0.121	0.20	1.46	0.256	0.03
0.22	0.91	23.1	0.63	0.110	0.20	1.34	0.234	0.06
0.37	1.32	33.5	0.64	0.112	0.18	1.31	0.230	0.03
0.34	1.43	36.3	0.57	0.101	0.21	1.22	0.213	0.06
0.45-A	1.86	47.2	0.60	0.104	0.17	1.20	0.211	0.03
0.45-B	1.96	49.8	0.54	0.095	0.20	1.12	0.197	0.06
0.54-A	2.43	61.7	0.55	0.096	0.17	1.10	0.192	0.02
0.54-B	2.47	62.7	0.54	0.094	0.18	1.08	0.189	0.03
0.52	2.48	63.0	0.51	0.089	0.20	1.05	0.184	0.06
0.61	2.99	75.9	0.48	0.084	0.21	0.99	0.173	0.05
0.65	3.00	76.2	0.49	0.086	0.20	0.99	0.173	0.02
0.67	3.01	76.5	0.50	0.088	0.19	1.01	0.177	0.02

PGA, peak ground acceleration.

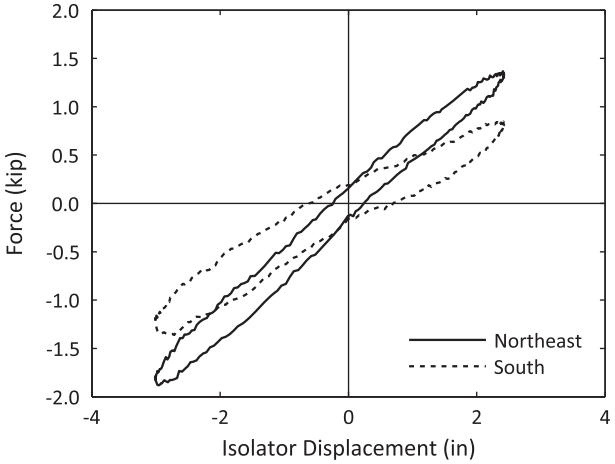

Figure 9. Comparison of the hysteresis loops from the El Centro record (PGA = 0.67 g) of the Northeast and South 40A isolators at a peak isolator displacement of 3.01 in. (76.5 mm).

DOI: 10.1002/stc

4.2. 50A isolators

The effective horizontal stiffness as a function of the peak isolator displacement obtained from the El Centro records is compared in Figure 10a. Similar to the 40A isolators, a softening trend occurs with increasing peak isolator displacement. At a peak isolator displacement of 0.39 in. (9.9 mm), the effective horizontal stiffness ranged between 1.66 kip/in. (0.291 kN/mm) and 1.74 kip/in. (0.305 kN/mm) for the Northwest and Southwest isolator, respectively. The effective horizontal stiffness decreased by 41% and 43% at 3.01 in. (76.5 mm) peak isolator displacement for the Northwest and Southwest isolator, respectively. A minimum effective horizontal stiffness of 0.97 kip/in. (0.170 kN/mm) was observed in the Northwest isolator. The variation in the effective horizontal stiffness was considerably lower in the 50A isolators than the 40A isolators. The c_v ranged between 0.02 and 0.06 in comparison with the range of 0.16 to 0.21 of the 40A isolators as shown in Table II.

The consistency of the equivalent viscous damping, compared in Figure 10b, is comparable with the consistency of the effective horizontal stiffness. In contrast to the 40A isolators, in which the damping generally increased with increasing peak displacement, the damping in the 50A isolators decreased slightly before increasing. A minimum damping of 5.2% in the Northwest isolator was observed at 1.32 in. (33.5 mm) peak isolator displacement in the 0.37 g PGA record. A maximum damping of 7.0% occurred at a peak isolator displacement of 3.01 in. (76.5 mm) in the Southwest isolator. Figure 11 compares the hysteresis loops of the Southwest and Northwest isolators. It can be observed that the hysteresis loops are comparable both in peak force and area contained within the loops, reinforcing the high consistency observed in the effective horizontal stiffness and damping.

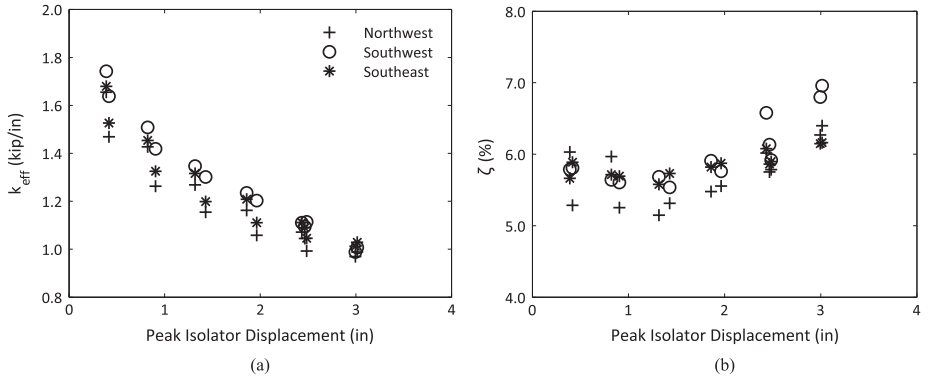

Figure 10. Comparison of the (a) effective horizontal stiffness and (b) the equivalent viscous damping as a function of peak isolator displacement obtained from the El Centro records for the 50A isolators.

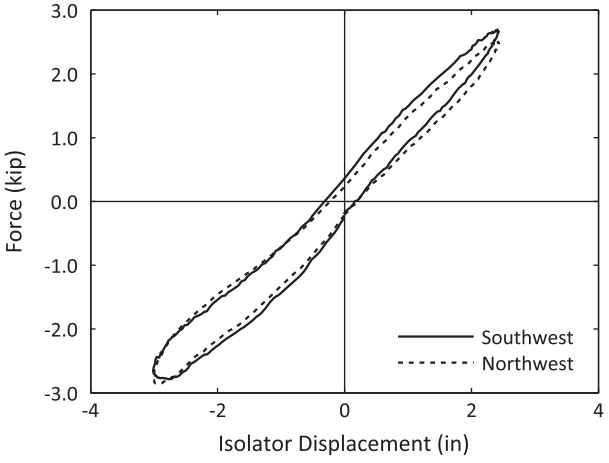

Figure 11. Comparison of the hysteresis loops from the El Centro record (PGA = 0.67 g) of the Northwest and Southwest 50A isolators at a peak isolator displacement of 3.01 in. (76.5 mm).

DOI: 10.1002/stc

5. COMPARISON BETWEEN ISOLATORS, THEN AND NOW

5.1. 40A isolators

From Kelly and Hodder [8], the average effective horizontal stiffness of a 40A isolator obtained during the El Centro record was 0.35 kip/in. (0.061 kN/mm) with 11.3% damping. Figure 12 compares the average hysteresis loop of a 40A isolator from Kelly and Hodder [8] to the hysteresis loop of the South isolator presented in this study. The hysteresis loop was selected from the 0.45 g-A record to approximately match the peak displacements of the cycle presented in the original study. It can be seen that significant stiffening occurred over the period despite the comparatively low effective horizontal stiffness of the South isolator. The effective horizontal stiffness of 0.49 kip/in. (0.086 kN/mm) was 40% greater than observed in the original study. The mean effective horizontal stiffness of the selected cycle was 0.60 kip/in. (0.105 kN/mm), an increase of 72%.

The equivalent viscous damping of the hysteresis loops in Figure 12 was approximately equal at 10.2% and 11.3% for the current and original study, respectively. Note that the South isolator was found to have significantly higher damping than either the North or Northeast isolator. Over the cycle presented in Figure 12, the damping was 6.2% and 5.4% in the North and Northeast isolator, respectively. The damping in the North and Northeast isolators decreased by 45% and 52%, respectively, in comparison with the 11.3% damping from the original study.

5.2. 50A isolators

The average effective horizontal stiffness of the 50A isolators from the El Centro record in Kelly and Hodder [8] was 0.66 kip/in. (0.116 kN/mm). Figure 13 compares the hysteresis loop from the original study to the Southwest isolator from the 0.54 g-A record highlighting the increase in effective horizontal stiffness. The effective horizontal stiffness in the Southwest isolator increased by 68% to 1.11 kip/in. (0.195 kN/mm). The mean effective horizontal stiffness of the selected cycle was 1.10 kip/in. (0.193 kN/mm), increasing by 67%. The damping decreased by a mean of 50% from 12.3% to 6.2%, which is comparable with the decrease observed in the North and Northeast 40A isolators.

5.3. Pullback tests

In the pullback tests conducted by Kelly and Hodder [8], the dynamic stiffness of the 40A and 50A isolators was 0.50 kip/in. (0.088 kN/mm) and 1.15 kip/in. (0.201 kN/mm), respectively. Table III shows the percent change of effective horizontal stiffness of the current study for each pullback test to the original study. The effective horizontal stiffness in the current study is obtained from the first full cycle of free vibration. The initial displacement in the original study was about 1 in. (25.4 mm). At this initial

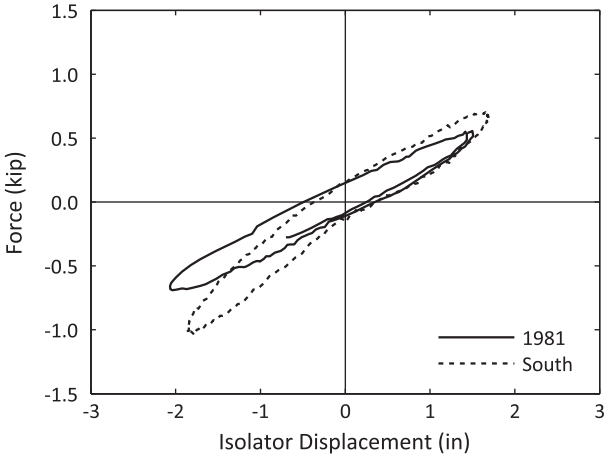

Figure 12. Comparison of the average hysteresis loops from the El Centro record of the 40A isolator presented in the original study and the South 40A isolator presented in the current study (PGA = 0.45 g-A).

DOI: 10.1002/stc

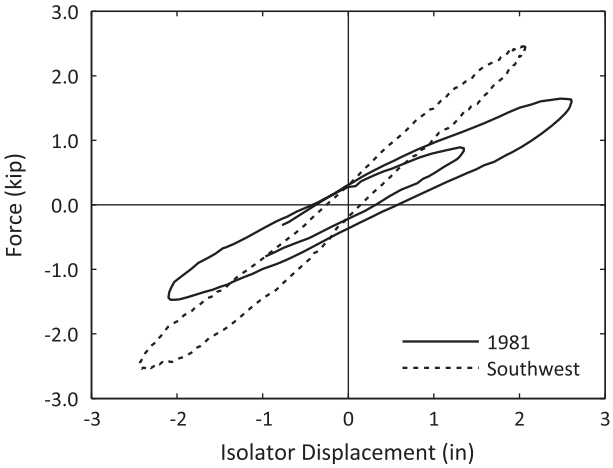

Figure 13. Comparison of the average hysteresis loops from the El Centro record of the 50A isolator presented in the original study and the Southwest 50A isolator presented in the current study (PGA = 0.54 g-A).

Table III. Percent change of the effective horizontal stiffness obtained from pullback tests.

Initial displacement		40A				50A			
(in.)	(mm)	North	South	Northeast	μ	Northwest	Southeast	Southwest	μ
1.0	25.4	53	16	68	45	24	29	33	29
1.2	30.5	41	5	63	36	21	26	30	26
1.5	38.1	34	2	56	31	15	20	23	19
1.5	38.1	24	−8	44	20	6	13	22	14
1.5	38.1	24	−8	44	20	6	13	22	14
1.5	38.1	22	−10	41	17	3	10	16	10
2.0	50.8	11	−21	32	7	−6	2	5	1

displacement, the effective horizontal stiffness of the 40A isolator increased between 16% and 68% for the South and Northeast 40A isolator, respectively. The mean increase was 45% and 29% for the 40A and 50A isolators, respectively.

As with the El Centro records, a general softening trend occurred as the initial displacement increased. Therefore, the percent change in Table III generally decreases with increasing initial displacement as the effective horizontal stiffness from the original study is constant. The effective horizontal stiffness of the South 40A isolator decreased below the original study at an initial displacement of 1.5 in. (38.1 mm). The mean effective horizontal stiffness of the 50A isolators at an initial displacement of 2.0 in. (50.8 mm) was approximately equal to the original study.

6. DISCUSSION

The increase in effective horizontal stiffness over the period was significantly larger than the stiffening observed in other studies of natural or accelerated aging such as Coladant [6] and Russo et al. [7]. The increase in effective horizontal stiffness was comparable with the accelerated aging results reported by Yura et al. [5] but observed in a considerably shorter period than predicted for natural aging at ambient temperature. It is postulated that the annular isolators considered in this study were more sensitive to aging because of the increased exposed surface from the unfilled core. If unfilled, the core of an annular isolator is an additional exterior surface that is susceptible to oxidation. It is anticipated that an annular isolator would be more sensitive to aging than an identical circular isolator because of a reduced interior region unaffected by the aging process. For the isolators considered, the maximum distance from an exposed edge was 0.88 in. (22.4 mm), which is significantly less than the 2.75 in. (69.9 mm)

DOI: 10.1002/stc

radius of an identical circular isolator. Therefore, the volume of elastomer protected from oxidation due to the reduced permeability of the oxidized surfaces is considerably less.

Note that the average vertical compressive force was 14.5 kip (64.5 kN) per isolator in comparison with 20.0 kip (89.0 kN) in the original study. It is known that the vertical compressive force is inversely proportional to the effective horizontal stiffness and proportional to the damping [9,11]. The effective horizontal stiffness is expected to decrease and the damping increase as the vertical compressive force increases. The damping is inversely proportional to the stiffness because of changes in the stored strain energy. Consequently, it is expected that the damping decreases with increasing stiffness.

From Naeim and Kelly [9], the horizontal stiffness using linear elastic analysis for SREIs is related to the vertical compressive force by

$$k_h = \frac{GA}{t_r}\left[1 - \left(\frac{P}{P_{crit}}\right)^2\right] \tag{1}$$

where k_h is the horizontal stiffness, G is the shear modulus of the elastomer, A is the shear area, t_r is the total thickness of the elastomeric layers, P is the vertical compressive force, and P_{crit} is the critical load.

The critical loads from the original study were 33.4 kip (149 kN) and 53.8 kip (239 kN) for the 40A and 50A isolators, respectively. It is expected that these values would also increase because of the stiffening of the elastomer from aging effects. Using the critical loads from the original study as a reference, from Eq. 1, the average vertical compressive force of 14.5 kip (64.5 kN) is not negligible, especially for the 40A isolators because of the lower critical load. Furthermore, review of the experimental results shows that the South 40A isolator was overloaded to approximately 25 kip (111 kN), whereas the Southeast and Southwest 50A isolators were approximately equally under loaded.

The effective horizontal stiffness from the 0.45 g-A record hysteresis loop increased by 40% in the South 40A isolator, which was overloaded, and a mean of 82% for the remaining two 40A isolators, which were under loaded in comparison with the original study. The large variation observed between the 40A isolators is in part attributed to the discrepancy in the vertical compressive force on the South 40A isolator in contrast to the approximately equally loaded North and Northeast isolators. The range of compressive force on the 40A isolators observed in the experiments brackets the average compressive force in the original study. Consequently, the increase in effective horizontal stiffness due to aging in the 40A isolators is expected to be between 40% and 82% if the compressive force between both experimental programs was consistent. The variation in the compressive force and the sensitivity of the 50A isolators to the compressive force was notably lower. Therefore, the increase in effective horizontal stiffness observed is primarily attributed to aging effects, although it is difficult to conclude the exact amount.

7. CONCLUSION

The sensitivity of the effective horizontal stiffness and equivalent viscous damping of Neoprene (Polychloroprene) SREIs to aging effects was investigated. Previously untested annular SREIs, of Shore A 40 durometer and 50 durometer hardness, were aged for over 30 years unloaded at room temperature. The bearings were compared with the findings of the original experimental program, conducted in 1981, through a series of similar shake table experiments on the bearings.

It has been demonstrated that significant variation occurred within the horizontal properties of the 40A isolators, whereas the variation within the 50A isolators was within acceptable limits. The peak displacement cycle from historical earthquake time histories with different levels of PGA were used to compare the effective horizontal stiffness and equivalent viscous damping. Both the 40A and 50A isolators exhibited a softening trend as the peak isolator displacement increased. The experimental results were compared by selecting a cycle with approximately equal displacements to the cycles presented in the original study. A significant mean increase in effective horizontal stiffness of 72% and 67% for the 40A and 50A isolators, respectively, was observed. Furthermore, with the exception of the South 40A isolator, the damping decreased by about 50%. A lower mean increase in effective horizontal stiffness of 45% and 29% for the 40A and 50A isolators, respectively, was observed by comparing the results of the pullback tests of the respective studies.

DOI: 10.1002/stc

The change in horizontal properties observed in this study was significantly larger or occurred over a shorter period than presented in other studies in the literature investigating Neoprene bearings with natural or accelerated aging. It was postulated that the increase in horizontal stiffness and decrease in damping were amplified because of the unfilled annular design of the isolator, which increases the exposed surface of isolator. In addition, it was noted that the vertical compressive force in the current study was less than in the original study, which is also associated with a higher effective horizontal stiffness. Despite the discrepancy in vertical compressive load, the changes in the properties of the isolators are primarily attributed to aging effects.

In light of the increase in effective horizontal stiffness and decrease in equivalent viscous damping, it is important to investigate the sensitivity of a base isolated structure to these changes. It is critical to determine if the performance of a base isolated structure with aged Neoprene elastomeric isolators is still within satisfactory limits.

ACKNOWLEDGEMENTS

This paper is based upon the work supported by the National Science Foundation under grant no. CMMI-0724208. Any opinions, findings, and conclusions expressed here are those of the authors and do not necessarily reflect the views of the National Science Foundation.

The authors thank T. Becker and B. Olson for the design and assembly of the model and S. Günay, S. Takhirov, and A. Schellenberg for their assistance in the experimental program. The support of the Natural Sciences and Engineering Research Council of Canada (NSERC) and a Vanier Canada Graduate Scholarship is gratefully acknowledged.

REFERENCES

1. Melkumyan MG. New Solutions in Seismic Isolation. Lusabats Publishing House: Yerevan, 2011.
2. Coladant C. Base isolation and aseismic bearings. In Recent Advances in Earthquake Engineering and Structural Dynamics, Davidovici V (ed). Ouest Editions: Nantes, 1992; 587–624.
3. ASTM International. Standard Test Method for Rubber—Deterioration by Heat and Oxygen, ASTM Standard D572-04. ASTM International: West Conshohocken, 2010.
4. Itoh Y, Gu HS. Prediction of aging characteristics in natural rubber bearings used in bridges. Journal of Bridge Engineering 2009; 14(2):122–128.
5. Yura J, Kumar A, Yakut A, Topkaya C, Becker E, Collingwood J. Elastomeric bridge bearings: recommended test methods, National Cooperative Highway Research Program Report No. 449. National Academy Press: Washington D.C., 2001.
6. Coladant C. Durability and ageing of elastomeric bearings in France. International Post-SMiRT Conference Seminar on Isolation, Energy Dissipation and Control of Vibrations of Structures, Italy, 1993.
7. Russo G, Pauletta M, Cortesia A. A Study on experimental shear behavior of fiber-reinforced elastomeric isolators with various fiber layouts, elastomers and aging conditions. Engineering Structures 2013; 52:422–433.
8. Kelly JM, Hodder SB. Experimental study of lead and elastomeric dampers for base isolation systems, Report No. UCB/EERC-81/16. University of California, Berkeley, 1981.
9. Naeim F, Kelly JM. Design of Seismic Isolated Structures: From Theory to Practice. Wiley: New York, 1999.
10. Buckle I, Nagarajaiah S, Ferrell K. Stability of elastomeric isolation bearings: experimental study. Journal of Structural Engineering 2002; 128(1):3–11.
11. Nagarajaiah S, Ferrell K. Stability of elastomeric seismic isolation bearings. Journal of Structural Engineering 1999; 125(9):946–954.

DOI: 10.1002/stc